Journal of
Materials Chemistry C

PAPER

View Article Online
View Journal

Cite this: DOI: 10.1039/c5tc00752f

Aggregation induced emission based fluorescence pH and temperature sensors: probing polymer interactions in poly(*N*-isopropyl acrylamide-*co*-tetra(phenyl)ethene acrylate)/poly(methacrylic acid) interpenetrating polymer networks†

Hui Zhou,[a] Feng Liu,[b] Xiaobai Wang,[a] Hong Yan,[a] Jing Song,[a] Qun Ye,[a] Ben Zhong Tang*[c] and Jianwei Xu*[a]

Received 17th March 2015,
Accepted 27th April 2015

DOI: 10.1039/c5tc00752f

www.rsc.org/MaterialsC

Aggregation induced emission (AIE) active copolymers **P1–P6** with high molecular weights (14 000–17 000) and low polydispersity indices (1.3–1.4) were prepared through copolymerization of *N*-isopropyl acrylamide (NIPAM) and tetra(phenyl)ethene (TPE)-based acrylate monomers. Copolymers **P1–P6** show comparable thermal stability to poly(*N*-isopropylacrylamide) (PNIPAM), while their glass transition temperatures are higher by 7–9 °C than those of pristine PNIPAM. Copolymers **P1–P6** are soluble in common organic solvents as well as in water. They retain a similar thermal sensitivity to PNIPAM, but their lower critical solution temperatures (LCST) are reduced with increase of TPE content. By changing the molar ratio of **P1–P6**/poly(methacrylic acid) (PMAA) and pH, complexes **P1–P6**–PMMA were studied by fluorescence spectroscopy and dynamic light scattering (DLS). The complexes are non-emissive in THF, and their fluorescence can be turned on upon addition of water. Moreover, their fluorescence is enhanced with the decrease in pH values due to the formation of interpenetrating polymer networks (IPNs) through inter-polymer hydrogen bonding. Fluorescence spectroscopy and DLS results also reveal that the phase transition behaviour of IPNs upon heating could be significantly modified by pH change. Reduction in the pH value from 7.0 to 4.0 leads to the decrease in LSCT of IPNs by up to 5 °C with respect to PNIPAM. By tuning the pH value to dissociate the formed inter-polymer hydrogen bonds, the formed IPNs would be able to fold cooperatively to a compact structure without a loss of solubility at temperatures below the LCST. Thus, these novel IPNs with AIE active moieties would be used as drug delivery systems, in which the release process could be readily monitored by fluorescence spectroscopy.

Introduction

Over the last few decades, dual or multi-responsive polymers have been receiving more attention with a special emphasis on the temperature and pH sensitiveness.[1] Polymer hydrogels are water-swollen polymer networks which are cross-linked through physical or chemical bonding. Some of the hydrogels exhibit sensitive response to external stimuli, such as pH and temperature. Due to their potential applications in biological systems, those hydrogels have been extensively investigated in many areas, such as controlled drug delivery,[2] molecular separation,[3] tissue culture substrates,[4] and enzyme activity controlling systems.[5]

Typically, copolymers with multi-responsive characteristics, which are usually prepared through copolymerization of at least two monomers with respective peculiarities, are employed to generate interpenetrating polymer networks (IPNs) with multi-responsive properties.[6] An alternative method has received more attention, in which the combined property can be easily tuned by chain interpenetration of two polymers with respective properties.[7] Each polymer retains its own property while proportion of each can be varied independently of the other, because there is no chemical bonding between two polymers.

Poly(methacrylic acid) (PMAA) is an ionizable hydrophilic polymer due to ionization/deionization of carboxylic acid groups, and thus its swelling behavior is greatly pH-dependent. Under low

[a] *Institute of Materials Research and Engineering, A*STAR (Agency for Science, Technology and Research), 3 Research Link, Singapore 117602, Republic of Singapore. E-mail: jw-xu@imre.a-star.edu.sg*
[b] *Department of Chemistry, National University of Singapore, 3 Science Drive 3, Singapore 117543, Republic of Singapore*
[c] *Department of Chemistry, The Hong Kong University of Science & Technology, Clear Water Bay, Kowloon, Hong Kong, China. E-mail: tangbenz@ust.hk*
† Electronic supplementary information (ESI) available. See DOI: 10.1039/c5tc00752f

pH conditions, –COOH groups are not ionized and cling to the PMAA network at its collapsed state through hydrogen bonding. While under high pH conditions, the –COOH groups are ionized and the charged $–COO^-$ groups repel each other, leading to PMAA swelling. Poly(*N*-isopropyl acrylamide) (PNIPAM) is a temperature-sensitive polymer, which shows drastic swelling transition at its lower critical solution temperature (LCST) of 32 °C.[8] At a low T (<32 °C) the gel is swollen, while at a high T (>32 °C) the polymer dehydrates to the collapsed state due to breakdown of the delicate hydrophilic/hydrophobic balance in the network structure. IPNs generated by PMAA and PNIPAM exhibited combined pH- and temperature-sensitivity. Due to the potential application in the real controlled drug delivery, the formation and interactions of such IPNs were investigated by several analytical methods, such as attenuated total reflectance Fourier transform infrared spectroscopy,[9] the viscometric method,[10] equilibrium swelling and oscillatory swelling studies,[11] and high-sensitivity differential scanning calorimetry.[12] However, those methods did not easily track the status of IPNs and thus were unable to real-time monitor the controlled drug delivery. The fluorescence methodology may be ideal for these purposes due to its ultrahigh sensitivity, superfast response and a convenient process.

Recently, although fluorescence probes have attracted increasing interest, the formation and interaction of IPNs formed from PMAA and PNIPAM have been rarely investigated by fluorescence spectroscopy mainly due to the lack of suitable luminogens, which exhibit sensitive response to external stimuli especially in an aqueous solution.[13] Several fluorophores, such as pyrene, rhodamine and tetraphenylethene (TPE), were covalently attached to PNIPAM chains to investigate their thermal transitions by fluorescence methodology. The fluorescence spectrum of the pyrene containing copolymer in general comprises monomer and excimer emissions, in which the ratio of these two types of emissions varies with temperature change.[14] The rhodamine system displays a temperature dependent fluorescence, which is caused by the PNIPAM dehydration at high temperatures under acidic conditions.[15] However, these common luminogens are not supreme models for the fluorescence probes since the aggregation-caused quenching effect is undesirable to a practical application, leading to reduction in efficiencies and sensitivities of sensors or probes. TPE is an unusual luminogen system in which aggregation works constructively rather than destructively in a conventional system, which exhibits high sensitivity to environmental changes, such as temperature, hydrophobicity and steric hindrance.[16] The emission is induced by aggregate formation, and thus this phenomenon is termed as aggregation induced emission (AIE). Due to the uniqueness of AIE luminogens that are emissive in the solid state, their applications in optoelectronics,[17] fluorescence sensors,[18] cell imaging,[19] and explosive chemical detection[20] have been paid increasing attention recently.

By covalently attaching TPE to the PNIPAN chain through a triazole linkage, PNIPAN displayed high fluorescence sensitivity on the thermally induced chain aggregation of PNIPAM under neutral conditions, which was used as a fluorescent thermometer to monitor the thermal transition of PNIPAM in water.[16a] While the conformation of the PNIPAM chain is very sensitive to its structure, even a subtle modification in the structure can lead to a huge change.[21] In order to minimize these negative effects, we here incorporated TPE with alkyl linkage into PNIPAM chains through copolymerization of monomers with TPE (**M1**–**M3**) and *N*-isopropyl acrylamide (NIPAM). The resultant copolymers could function as a fluorescence probe to track the interaction of PMAA and PNIPAM during IPN formation under different conditions, including pH, the component ratio and temperature.

Experimental

General

All synthetic manipulations were carried out under an atmosphere of dry argon gas using standard vacuum-line Schlenk techniques. All solvents were degassed and purified before use according to standard literature methods. Diethyl ether, hexanes, tetrahydrofuran, and toluene were purchased from Aldrich Chemical Co. Inc. and distilled from sodium/benzophenone ketyl before use.

Materials

NIPAM was purchased from Aldrich and purified by crystallization before use. 2,2′-Azoisobutyronitrile (AIBN) was purchased from Aldrich and purified by crystallization before use. Other commercially available reagents and solvents were used as received. PMAA was purchased from Aldrich, and the molecular weight is 9.5 kDa according to GPC.

Instrumentation

^1H and ^{13}C nuclear magnetic resonance (NMR) spectra were recorded on a Bruker DRX 400 MHz NMR spectrometer in $CDCl_3$ at room temperature using tetramethylsilane (TMS) as an internal standard. Operating frequencies of the NMR spectrometer were 400.13 MHz (^1H) and 100.61 MHz (^{13}C). High resolution MS (HRMS) were recorded using a Micromass 7034E mass spectrometer. Elemental analysis was conducted on a Perkin-Elmer 240C elemental analyzer for C, H, and N determination. UV-vis and fluorescence spectra were obtained using a Shimadzu UV3101PC UV-vis-NIR spectrophotometer and a Perkin-Elmer LS 50B luminescence spectrometer with a Xenon lamp as a light source, respectively. Thermal analysis was performed on a Perkin-Elmer thermogravimetric analyzer (TGA 7) in nitrogen or in air at a heating rate of 20 °C min^{-1} and on a TA Instruments Differential Scanning Calorimetry (DSC) 2920 at a heating rate and a cooling rate of 5 °C min^{-1} in nitrogen. Dynamic light scattering experiments were performed on a Brookhaven 90 plus spectrometer with a temperature controller. An argon ion laser operating at 633 nm was used as a light source.

Preparation of interpolymer complexes

Stock solutions of copolymers and PMAA in a water or buffer solution were used for the preparation of inter-polymer complexes. They were prepared by a drop wise addition of the PMAA stock solution to copolymer stock solution under continuous stirring.

The mixtures were incubated at room temperature for 1 day prior to the experiment. Polymer composition in the complexes was presented by the polymer molar ratio *r*, *i.e.*, the ratio of molar concentrations of PNIPAM and PMAA. An inter-polymer composition of the copolymer was kept constant as 0.50 mg mL^{-1}. The pH of the complexes was varied by using appropriate buffer solutions: a 10 mM buffer system of sodium phosphate and citric acid, pH ranging from 2.8 to 7.0.

Synthesis of compounds and polymers

4-(1,2,2-Triphenylvinyl)phenyl acrylate (M1). 4-(1,2,2-Triphenylvinyl)phenol (522.6 mg, 1.5 mmol) was dissolved in dry dichloromethane (10.0 mL). After adding 3.0 equiv. of triethylamine (607.0 μL, 4.5 mmol) to the solution, 2.0 equiv. of acryloyl chloride (235.0 μL, 3.0 mmol) were added drop wise at 0 °C. The mixture was then stirred at room temperature for 4 h. The ammonia salts were filtered off and the solvent was evaporated. The crude product was purified on a silica gel using column chromatography with a dichloromethane and hexane (1 : 2) mixture as the eluent, giving the desired product as white solids of 567.8 mg (yield: 94.0%). ^{1}H NMR ($CDCl_3$): δ 7.14–7.06 (m, 17H), 6.91 (d, 2H, J = 8.0 Hz), 6.58 (d, 1H, J = 16.8 Hz), 6.30 (dd, 1H, J = 6.8, 10.5 Hz), 5.99 (d, 1H, J = 10.5 Hz). ^{13}C NMR ($CDCl_3$): δ 164.2, 149.1, 143.7, 143.6, 141.5, 141.4, 140.1, 132.5, 132.4, 131.5, 131.4, 128.1, 127.9, 127.8, 126.7, 126.6, 120.8. IR (thin film): ν = 3075, 3049, 3120, 2924, 1952, 1903, 1805, 1745, 1739, 1638, 1598, 1503, 1492, 1443, 1297, 1248, 1199, 1170, 1147, 1022, 997, 902, 764, 753, 701, 614 cm^{-1}. HRMS (ESI†): [M + Na^+] calcd for $C_{29}H_{22}O_2Na$, *m*/*z* 425.1517; found, *m*/*z* 425.1534.

General procedure for copolymerization

All polymers were prepared by free radical polymerization of the corresponding monomers in the presence of AIBN. A solution of 0.50 mmol of monomers and 1.5 mg of AIBN dissolved in 1.0 mL of dry THF was degassed by three freeze/thaw cycles. The solutions were stirred for 48 h at 70 °C in sealed vessels. The reaction mixture was added dropwise into diethyl ether with stirring, and then the precipitate was collected by filtration. This purification process was repeated several times to ensure that all unreacted starting materials were removed. The polymer was re-dissolved in 5.0 mL of THF and re-precipitated with Et_2O to afford a white solid. The polymer was then filtered and dried under vacuum at 40 °C for 72 hours for further analysis.

Copolymer P1. Yield: 85%; ^{1}H NMR ($CDCl_3$): δ 3.99–3.88 (m, 2H), 2.23–1.40 (m, 3H), 1.14 (s, 6H). Anal. calcd for $(C_6H_{11}NO)_n$: C, 63.69; H, 9.80; N, 12.38. Found: C, 63.74; H, 9.68; N, 12.37. IR (thin film): ν = 3436, 3300, 3077, 2974, 2936, 2877, 1651, 1548, 1459, 1388, 1368, 1276, 1172, 1131, 701 cm^{-1}.

Copolymer P2. Yield: 87%; ^{1}H NMR ($CDCl_3$): δ 3.99–3.73 (m, 2H), 2.23–1.40 (m, 3H), 1.14 (s, 6H). Anal. calcd for $(C_6H_{11}NO)_n$: C, 63.69; H, 9.80; N, 12.38. Found: C, 63.73; H, 9.82; N, 12.36. IR (thin film): ν = 3437, 3299, 3077, 2974, 2936, 2877, 1651, 1549, 1459, 1388, 1368, 1277, 1173, 1131, 702 cm^{-1}.

Copolymer P3. Yield: 84%; ^{1}H NMR ($CDCl_3$): δ 3.99 (br, 2H), 2.23–1.40 (m, 3H), 1.14 (s, 6H). Anal. calcd for $(C_6H_{11}NO)_n$: C, 63.69; H, 9.80; N, 12.38. Found: C, 63.72; H, 9.81; N, 12.37. IR (thin film): ν = 3440, 3301, 3077, 2975, 2936, 2877, 1652, 1549, 1459, 1388, 1368, 1277, 1173, 1131, 701 cm^{-1}.

Copolymer P4. Yield: 88%; ^{1}H NMR ($CDCl_3$): δ 3.99 (br, 2H), 2.23–1.40 (m, 3H), 1.14 (s, 6H). Anal. calcd for $(C_6H_{11}NO)_n$: C, 63.69; H, 9.80; N, 12.38. Found: C, 63.70; H, 9.82; N, 12.38. IR (thin film): ν = 3441, 3300, 3077, 2975, 2937, 2877, 1652, 1550, 1459, 1388, 1368, 1278, 1173, 1131, 701 cm^{-1}.

Copolymer P5. Yield: 79%; ^{1}H NMR ($CDCl_3$): δ 3.99–3.88 (m, 2H), 2.26–1.43 (m, 3H), 1.14 (s, 6H). Anal. calcd for $(C_6H_{11}NO)_n$: C, 63.69; H, 9.80; N, 12.38. Found: C, 63.71; H, 9.83; N, 12.37. IR (thin film): ν = 3441, 3299, 3080, 2975, 2937, 2877, 1647, 1551, 1460, 1388, 1369, 1280, 1244, 1173, 1132, 701, 668 cm^{-1}.

Copolymer P6. Yield: 86%; ^{1}H NMR ($CDCl_3$): δ 3.98 (s, 1H), 3.56 (s, 2H) 2.26–1.43 (m, 2H), 1.14 (s, 6H). Anal. calcd for $(C_6H_{11}NO)_n$: C, 63.69; H, 9.80; N, 12.38. Found: C, 63.70; H, 9.81; N, 12.36. IR (thin film): ν = 3438, 3300, 3081, 2975, 2937, 2878, 1650, 1550, 1459, 1389, 1369, 1336, 1280, 1245, 1173, 1132, 701, 668 cm^{-1}.

Results and discussion

Synthesis and characterization of monomers and related copolymers

The synthetic routes leading to copolymers **P1–P6** are shown in Scheme 1. **M1** could be prepared in a yield of 94% by the reaction of 4-(1,2,2-triphenylvinyl)phenol with acryloyl chloride in the presence of triethylamine in dry dichloromethane. Monomers **M2** and **M3** were prepared according to our previous work (Scheme S1, ESI†).[20a,b] Poly(*N*-isopropyl acrylamide-*co*-tetra(phenyl)ethene acrylate) **P1–P6** were prepared from a mixture of monomers **M1–M3** and NIPAM in different ratios by radical polymerization using AIBN as a radical initiator. **P1–P6** were purified by re-precipitation twice in diethyl ether to give white solids with 79–85% isolated yields.

P1–P6 are not only soluble in many common organic solvents, such as tetrahydrofuran (THF), dichloromethane, chloroform, methanol and dimethyl sulfoxide (DMSO), but also in water. **P1–P6** were structurally characterized by various spectroscopic methods and elemental analysis. Using **P1** as an example, the

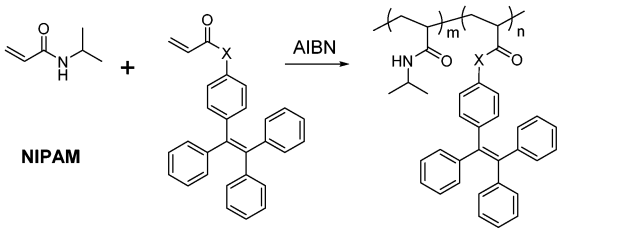

M1: X = O;
M2: X = $O(CH_2)_6O$;
M3: X = $O(CH_2)_{12}O$

P1: X = O; m = 96, n = 1
P2: X = O; m = 211, n = 1
P3: X = O; m = 357, n = 1
P4: X = O; m = 438, n = 1
P5: X = $O(CH_2)_6O$; m = 411, n = 1
P6: X = $O(CH_2)_{12}O$; m = 419, n = 1
The ratio of m to n was determined by the UV-vis absorption spectra.

Scheme 1 Synthetic route of monomer copolymers (**P1–P6**).

Table 1 Molecular weight, polydispersity (PDI) and thermal data of PNIPAM and **P1–P6**[a]

Polymers	Feed ratio $x:y$	Experimental $m:n$	M_w (10^4)	M_n (10^4)	PDI	T_d[b]	T_g
PNIPAM	—	—	1.48	1.01	1.4	357	130
P1	100 : 1	96 : 1	1.62	1.23	1.3	361	138
P2	200 : 1	211 : 1	1.46	1.13	1.3	360	137
P3	300 : 1	357 : 1	1.49	1.15	1.3	357	138
P4	400 : 1	438 : 1	1.60	1.18	1.4	359	139
P5	400 : 1	411 : 1	1.63	1.19	1.4	360	138
P6	400 : 1	419 : 1	1.61	1.19	1.4	361	140

[a] M_w: the weight-average molecular weight. M_n: the number-average molecular weight. [b] T_d: the decomposition temperature at which 5% weight loss occurs.

^{1}H NMR spectrum of **P1** is illustrated in Fig. S1 (ESI†). The presence of signals at δ 7.00–6.52 corresponding to protons of TPE indicated that the TPE residues remained intact during the radical polymerization and purification process. The molecular weights of these copolymers against polystyrene standards were determined by gel permeation chromatography (GPC) and the data are summarized in Table 1. **P1–P6** have high molecular weights of 14 600–16 300 with a relatively narrow polydispersity index of 1.3–1.4. Those polymers exhibit high thermal stability with decomposition temperatures ranging from 357 to 361 °C under nitrogen, which are comparable to 357 °C of PNIPAM (Fig. S2a, ESI†). The DSC study indicates that **P1–P6** exhibit a glass transition temperature of 138–140 °C under nitrogen, which is slightly higher than that of PNIPAM ($\Delta T_g > 7$ °C, ESI,† Fig. S2b). The ratio of TPE to NIPAM was determined by UV-vis absorption spectra (ESI,† Fig. S3).

AIE properties of copolymers

P1–P6 were non-emissive when dissolved in THF, which is a good solvent for both TPE and NIPAM. **P1–P6** with different degrees of TPE labelling also showed similar AIE properties. Taking **P4** solution in THF as an example (Fig. S4, ESI†), the fluorescence started to become obvious when a large amount of H_2O (>70%) was added, indicating that TPE maintained its AIE activity after being incorporated into the polymer NIPAM, which was further evidenced by the strong emission of films fabricated from **P1–P6** and **M1–M3** (ESI,† Fig. S5). When compared to **P1–P6** films, obvious red-shifts (4–6 nm) in emission spectra were found for the **M1–M3** films, implying their better stacking in the solid state. The AIE property of the **P4**–PMAA complex in a THF/H_2O mixture was studied. As shown in Fig. 1, the mixture showed very good solubility in pure THF and was non-emissive. While increasing water content, the fluorescence could be turned on when water content is 60%, and finally reached the maximum fluorescence intensity in 100% water. The **P4**–PMAA complex showed similar AIE properties to **P4**, but emitted 1.5-fold stronger fluorescence than that of neat **P4** with the same concentration, because the polymer interaction suppressed the molecular motions of TPE.[16a] Another possibility to restrict the TPE motion is that the entangling of polymer chains may lead to the enhancement in fluorescence. No obvious increase in fluorescence intensity in a non-hydrogen-bonded system **P4**/polystyrene indicates that entangling of polymer chains has no effect on the fluorescence enhancement (ESI,† Fig. S6).

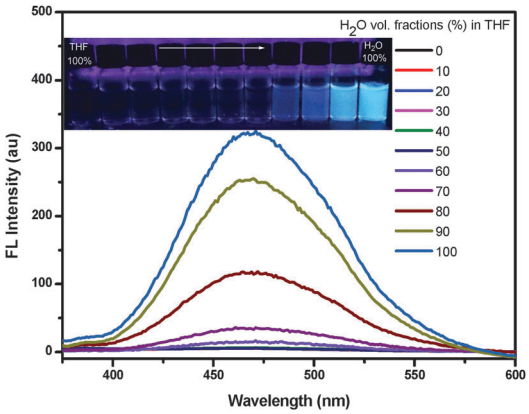

Fig. 1 Fluorescence spectra of **P4**/PMAA in THF/H_2O; λ_{ex} = 318 nm; [**P4**] = 0.5 mg mL^{-1}, 5.0 equiv. of PMAA, 20 °C, inserts are photographs of **P4**/PMAA solutions taken under UV illumination (365 nm).

Considering the good fluorescence response of TPE to the phase change of the polymer chain, TPE could be used as a fluorescence probe to investigate the formation of hydrogen bonds in PMAA and PNIPAM interpenetrating polymer networks.

The thermally induced fluorescence of copolymers

Fig. 2a shows the effect of temperature on **P1–P6** fluorescence in an aqueous solution. Taking **P4** for example, a small change in the emission intensity was observed when **P4** was heated from 14.0 to 25.0 °C, and a continuous increase in fluorescence intensity was recorded in the range of 25.0 to 30.0 °C, finally the fluorescence intensity reached the maximum at 32.5 °C. Further heating to 50.0 °C led to no change in the fluorescence intensity. When cooled down from 50.0 to 14.0 °C, a reversible temperature-dependent fluorescence curve was obtained with the same trend in the same temperature regions (ESI,† Fig. S6a). This phenomenon is supported by dynamic light scattering (DLS) and solution turbidity measurements (Fig. 2b and Fig. S6b, ESI†), which show the reversible temperature-dependent particle size and solution turbidity curves, implying that **P4** chains swell well in water at the beginning and start to collapse at 22.5 °C due to dehydration, and the particle reaches the smallest size at 32.5 °C.

As shown in Fig. 2, **P1–P3** with a higher degree of labeled TPE display down-shift LSCT and easily precipitate out when heating. It is well known that the conformation of the PNIPAM chain is very sensitive to its structure, and even a subtle modification in the structure can result in a huge change.[21] Thus, by tuning the degree of labelled TPE, the conformation of the PNIPAM chain could be modified well, and **P4–P6** with a very low degree of labeled TPE keep the similar conformation of PNIPAM.

The starting point of fluorescence enhancement for **P4** relates slightly to its concentration, *e.g.* from 0.1 to 1.0 mg mL^{-1} (ESI,† Fig. S7). However, the fluorescence intensity of polymers with a higher concentration, such as 1.0 mg mL^{-1} solution, decreased swiftly on heating from 37.0 to 50.0 °C, due to their precipitation at

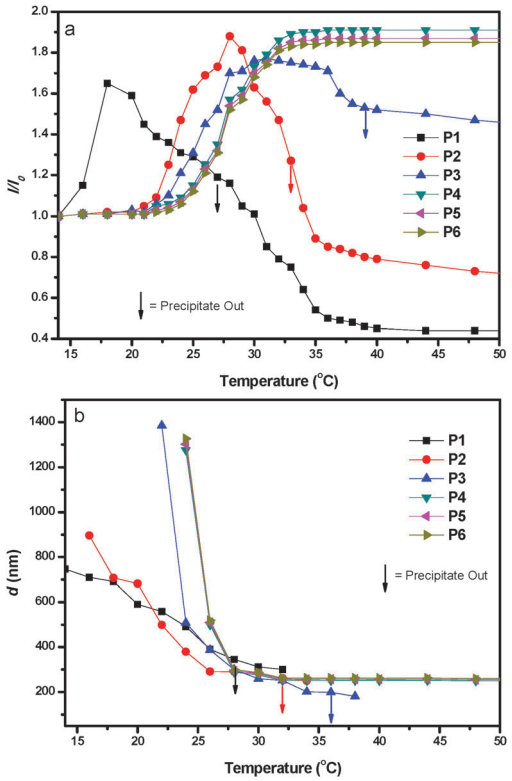

Fig. 2 (a) Plot of I/I_0 *vs.* temperature of **P1–P6** in H_2O. (b) The particle size *vs.* temperature of **P1–P6** in H_2O. The concentration of the polymer is 0.50 mg mL^{-1}, I_0 = intensity at 469 nm at 14 °C, excited at 318 nm.

a higher temperature than LCST. Moreover, as shown in Fig. 2, **P1–P3** with higher TPE labeling degrees showed lower LSCT of 30.0, 28.5 and 18.0 °C, respectively. As the hydrophobic interaction between the TPE residues may enable the aggregation of TPE, this likely promotes the hydrophobic backbones of PNIPAM chains to conglobulate.[16a] While **P5** and **P6** functioned similarly as **P4**, and the LSCTs were not changed, although TPE was attached to the PNIPAM chain through an alkyl linkage. Thus, **P4–P6** with a lowest degree of TPE maintained the same LSCT as that of PNIPAM, and the LSCT of copolymers could be tuned by adjusting the degree of TPE residues in copolymers.

Formation of interpenetrating polymer networks

Scheme 2 illustrates the hydrogen bond formation in IPNs formed by **P4** and PMAA. The formation and interaction of hydrogen bonds between PMAA and **P4** was investigated by fluorescence spectroscopy in the pH range of 2.8–7.0, and the concentration of **P4** was set as 0.50 mg mL^{-1}. Fig. 3a summarizes the fluorescence spectra of the PMAA–**P4** complex with different compositions at pH 2.8, 3.4, 4.0, 4.6, 5.2 and 7.0, respectively. Pronounced changes in the fluorescence intensity were observed upon PMAA addition at pH values less than 5.2, and fluorescence was further enhanced until the ratio of PMAA and polymer (r) is 3.0. As shown in Fig. 3b, the fluorescence enhancement fold reached a maximum of 1.93 at pH 2.8. When the pH was increased to 7.0, fluorescence enhancement was not observed even with the addition of high excess of PMAA

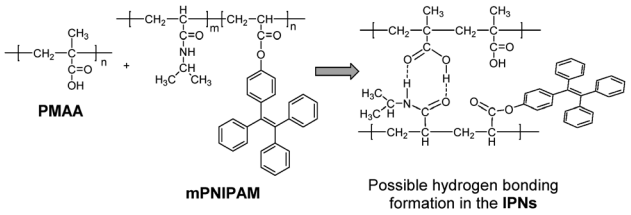

Scheme 2 The illustration of PMAA, PNIPAM and the hydrogen-bond formation between the two networks in the IPNs.

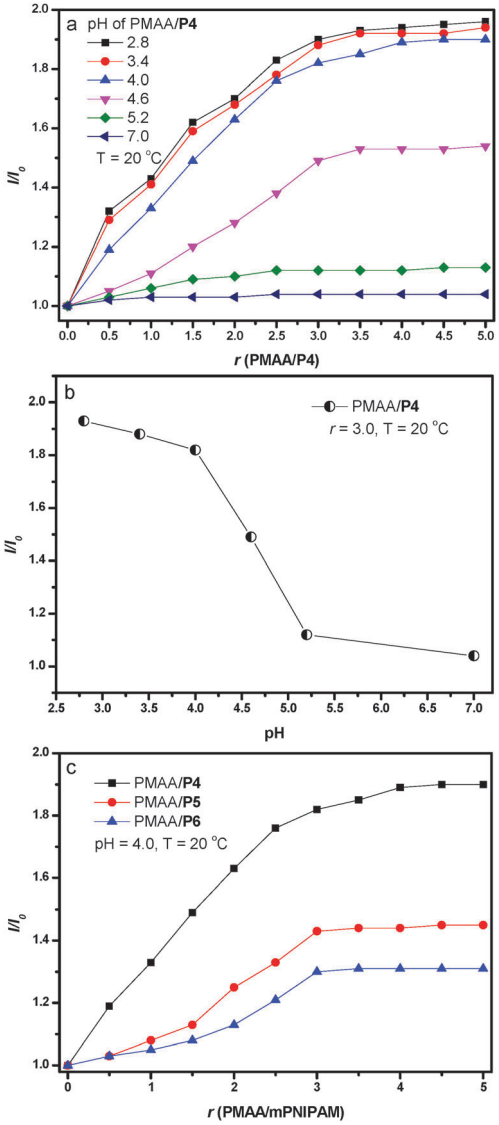

Fig. 3 (a) Plot of I/I_0 *vs.* ratio of PMMA and **P4** at different pH, r = 0–5.0, pH = 2.8–7.0. (b) Plot of I/I_0 *vs.* pH at r = 3.0. (c) Plot of I/I_0 *vs.* ratio of PMMA and **P4–P6** at pH = 4.0. [Copolymer] = 0.5 mg mL^{-1}, 10.0 mM Na_2HPO_4–citric acid buffer, I_0 = intensity at 469 nm at 20 °C, λ_{ex} = 318 nm.

(*ca.* 10-fold), suggesting that no strong interaction takes place between **P4** and PMAA. In other words, no inter-polymer complexes are formed between **P4** and PMAA although mixed in the solution. This phenomenon could be related to the high ionization degree of PMAA at pH 7.0 that it is not able to form

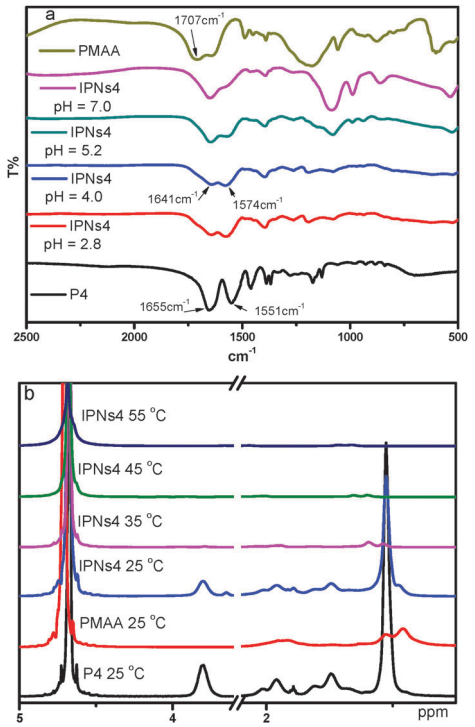

Fig. 4 (a) FTIR spectra of solid **P4** and IPNs4 under different pH conditions. IPNs4 solid samples were prepared from solutions by freeze drying to remove water. (b) ^{1}H NMR spectra of **P4**, PMAA and IPNs4 in D_2O at various temperatures, [**P4**] = 0.50 mg mL^{-1}, r = 3.0.

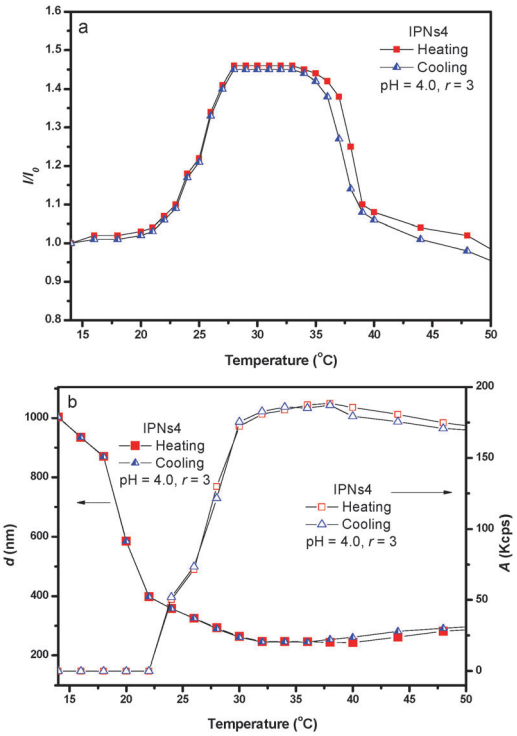

Fig. 5 (a) Plot of I/I_0 *vs.* temperature of IPNs4 during a heating and cooling cycle at pH = 4 and r = 3. (b) The particle size and solution turbidity (kcps) *vs.* temperature of IPNs4. [**P4**] = 0.50 mg mL^{-1}, r = 3.0, pH = 4.0, 10.0 mM Na_2HPO_4–citric acid buffer. I_0 = intensity at 469 nm at 14 °C, λ_{ex} = 318 nm.

hydrogen bonds with PNIPAM, because PMAA has a related low pK_{int} of 4.85.[22] All fluorescence changes occurred in a narrow range of r from 1.0 to 3.0, indicative of the cooperative character of IPNs4 formation. However, **P5** and **P6** labeled with TPE units through a longer alkyl chain displayed much lower fluorescence enhancement upon PMAA addition (Fig. 3c). FTIR spectra was widely used to verify the formation of hydrogen bonds.[23] Using **P4** and its IPNs as examples, FTIR spectra of **P4**, PMAA and IPNs4 at different pH values were studied. As shown in Fig. 4a, the peak at 1707 cm^{-1} represents the carbonyl (–C═O) stretching vibration in the carboxylic acid groups of PMAA. The peaks at 1655 and 1551 cm^{-1} belong to –C═O stretching vibration and –N–H deformation in the amide groups in **P4**, respectively. Their mixture, for example, IPNs4 at pH 4.0, exhibits two signals at 1641 and 1574 cm^{-1}, corresponding to the red-shifted –C═O stretching vibration of carboxylic acid and the amide group of **P4**, and blue-shifted –N–H deformation in the amide group, indicating the formation of hydrogen bonds between **P4** and PMAA.

The temperature dependent fluorescence transition of IPNs4 at a constant mixture composition (r = 3.0, Fig. 5a) was examined. At pH 4.0, a noticeable difference in the fluorescence trend was observed, which could be split into three stages. A big bump in the emission intensity of IPNs4 was found when it is heated from 20.0 to 27.5 °C, and the fluorescence intensity reached the maximum at 27.5 °C. In the range from 27.5 to 35.0 °C, a stable fluorescence intensity region was recorded, indicating its thermal tolerance during this temperature range. While further heating to 50 °C, a continuous decrease in fluorescence density was observed due to thermally activated molecular motions of TPE,[16a] which was supported by the DLS results that particle sizes became smaller but no precipitation was produced during this heating process (Fig. 5b). When cooled down from 50.0 to 14.0 °C, a coincided fluorescence intensity–temperature curve and a particle size curve were obtained, implying its good thermal reversibility. The fluorescence and DLS measurements showed the LCST of IPNs4 at 27.5 °C, which was 5.0 °C lower than that of **P4**. The ^{1}H NMR spectra of IPNs4 are measured in D_2O at various temperatures to give insight into its thermal transitions (Fig. 4b). IPNs4 start to dehydrate at 25 °C but still swell well in H_2O. The protons chains could be identified in the ^{1}H NMR spectra when the temperature is at 25 °C. However, when IPNs4 solution is heated up to 35 °C or higher, IPNs4 collapse to form compact particles and thus lead to a gradual decrease in intensity of NMR peaks.

IPNs4 particles under different pH and temperatures were examined (Fig. 6). IPNs4 particles with a bright blue emission, which resemble the stars in the galaxy, could be clearly observed upon excitation with UV light (excitation wavelength: 378 nm). Fig. 6c, g and h display IPNs4 particles at 20, 35 and 50 °C, respectively, which is consistent with observations in Fig. 5a. Under low pH (2.8, 3.4 and 4.0), IPNs4 formed crystal-like particles with strong fluorescence emission due to the more efficient hydrogen bonding at a lower pH. While at a

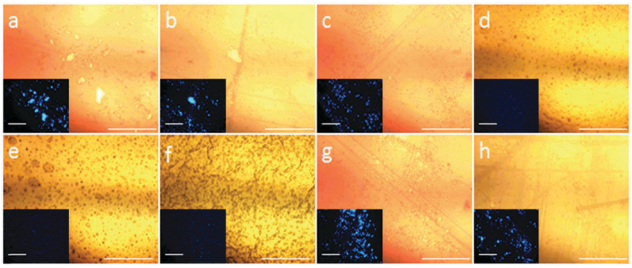

Fig. 6 Optical microscopy images and fluorescence microscopy images (inserted photos) of IPNs4 particles under different pH and temperatures: (a) 2.8, 20 °C; (b) 3.4, 20 °C; (c) 4.0, 20 °C; (d) 4.6, 20 °C; (e) 5.2, 20 °C; (f) 7.0, 20 °C; (g) 4.0, 35 °C; and (h) 4.0, 50 °C. The fluorescence microscopy images of particles were taken using a fluorescence microscope with a 337 nm excitation; scale bar is 50 μm. [**P4**] = 0.50 mg mL^{-1}, r = 3.0, 10.0 mM Na_2HPO_4–citric acid buffer.

higher pH than 4.0, IPNs4 become amorphous and emitted less fluorescence.

At higher pH values than pK_{int} (4.85) as shown in Fig. 7a, IPNs4 tend to display similar fluorescence behavior to **P4** because of the weaker hydrogen bonding interaction caused by ionization in different degrees of PMAA. On the other hand, a decrease in pH from 7.0 to 4.6 led to a gentle reduction in LSCT from 32.5 to 29.0 °C. For pH 3.4 and 2.8, IPNs4 showed a slight opalescence and started to precipitate out on heating up to 28.0 °C (Fig. 7b).

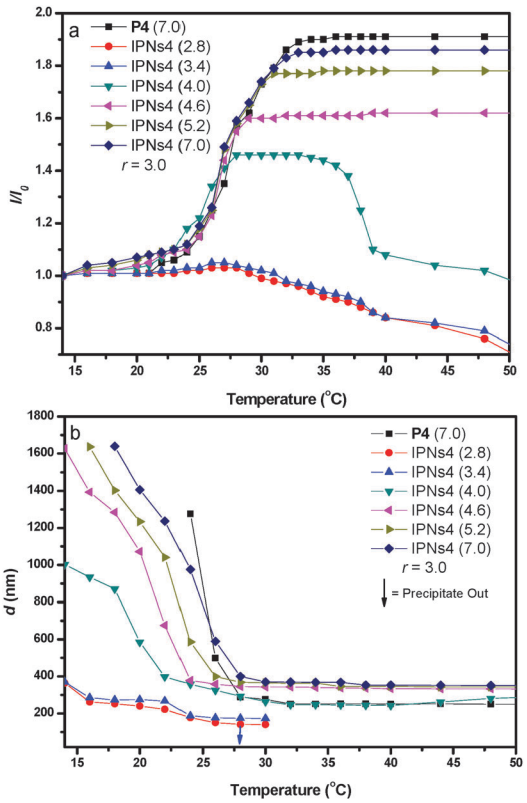

Fig. 7 (a) Plot of I/I_0 *vs.* temperature of IPNs4. (b) Plot of the particle size of IPNs4 *vs.* temperature. [**P4**] = 0.50 g mL^{-1}, r = 3.0, pH = 2.8–7.0, 10.0 mM Na_2HPO_4–citric acid buffer. I_0 = intensity at 469 nm at 14 °C, λ_{ex} = 318 nm.

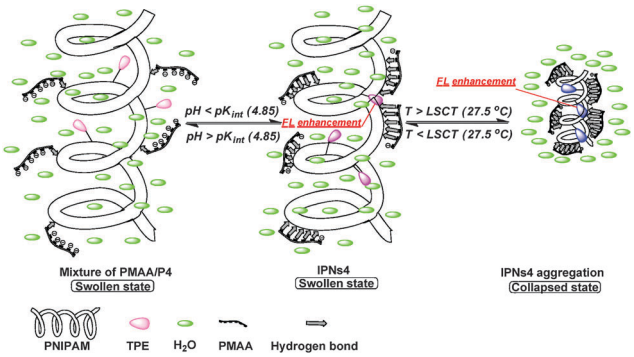

Fig. 8 Schematic illustration of the structures of **P4**–PMAA complexes at different pH and temperatures.

Considering the down-shift LSCT together with the fluorescence transition, the effect of mixture composition and the pH value on the structure of IPNs4 is illustrated in Fig. 8. When pH (7.0 and 5.2) > pK_{int}, less hydrogen bonds between PMAA and PNIPAM were formed because most of the carboxylic groups in PMAA were ionized. Even when the PMAA content in a mixture was very high (for example, r = 10.0), LCST of PNIPAM changed only slightly. In this case, the length of the hydrophobic PNIPAM blocks in the complexes was long enough to provide high cooperativity of the phase transition of PNIPAM, and thus fluorescence transitions of mixtures show similar trends to **P4**. At pH (4.6, 4.0, 3.4 and 2.8) < pK_{int}, due to the fact that more carboxylic groups in PMAA were protonated, more hydrogen bonds between PNIPAM were generated to form IPNs4. Under this condition, the phase transition of PNIPAM will be affected even though the PMAA content is low. In the IPNs4 complex, the hydrophobic blocks are much shorter, consequently resulting in the low transition cooperativity. Thus, the down shifts of LSCT for IPNs4 were observed with an increase in pH values.

Overall, the ionized PMAA chains introduced more changes to the mixture of PMAA–**P4**, which improved the solubility of IPNs4 and maintained the cooperativity of phase transition of **P4**. In contrast, PNIPAM chains could be hydrophilized by conjugation with more hydrophilic PMAA to generate IPNs4 through the formation of hydrogen bonding, leading to a decrease in LSCT and **P4** lost its original features as that of PNIPAM.

Conclusions

In summary, a new type of IPNs was formed through the intermolecular hydrogen bonding interaction between PMAA and PNIPAM containing AIE active TPE. The TPE moieties that were covalently linked to the PNIPAM chain displayed highly sensitive response to the phase transition of IPNs, which could be used as a fluorescence probe to track the IPNs' structural changes caused by external pH and temperature. By adjusting pH, the formed IPNs would be able to fold cooperatively to a compact structure without a loss of solubility at temperatures below the LCST. Thus, these IPNs would be used as convenient drug delivery systems, in which the release process can be monitored by fluorescence spectroscopy *in situ*.

Acknowledgements

The authors would like to acknowledge the financial support (Grant No: 1321760011) from the Institute of Materials Research and Engineering (IMRE), Agency for Science, Technology and Research (A*STAR).

Notes and references

1 (*a*) C. M. Chopko, E. L. Lowden, A. C. Engler, L. G. Griffith and P. T. Hammond, *ACS Macro Lett.*, 2012, **1**, 727; (*b*) C. Zhang and M. Maric, *J. Polym. Sci., Part A: Polym. Chem.*, 2012, **50**, 4341; (*c*) D. Fournier, R. Hoogenboom, H. M. L. Thijs, R. M. Paulus and U. S. Schubert, *Macromolecules*, 2007, **40**, 915; (*d*) B. S. Lokitz, A. W. York, J. E. Stempka, N. D. Treat, Y. Li, W. L. Jarrett and C. L. McCormick, *Macromolecules*, 2007, **40**, 6473.

2 (*a*) J. Zhang, L. Wu, F. Meng, Z. Wang, C. Deng, H. Liu and Z. Zhong, *Langmuir*, 2012, **28**, 2056; (*b*) D. Schmaljohann, *Adv. Drug Delivery Rev.*, 2006, **58**, 1655; (*c*) C. Ramkissoon-Ganorkar, A. Gutowska, F. Liu, M. Baudys and S. W. Kim, *Pharm. Res.*, 1999, **16**, 819.

3 H. Feil, Y. H. Bae, J. Feijen and S. W. Kim, *J. Membr. Sci.*, 1991, **64**, 283.

4 T. Takezawa, Y. Mori and K. Yoshizato, *Biotechnology*, 1990, **8**, 854.

5 F. Liu, G. L. Tao and R. X. Zhuo, *Polym. J.*, 1993, **25**, 561.

6 (*a*) P. Shi, Q. Li, X. He, S. Li, P. Sun and W. Zhang, *Macromolecules*, 2014, **47**, 7442; (*b*) R. T. Pearson, N. J. Warren, A. L. Lewis, S. P. Armes and G. Battaglia, *Macromolecules*, 2013, **46**, 1400; (*c*) K. Bauri, S. Pant, S. G. Roy and P. De, *Polym. Chem.*, 2013, **4**, 4052; (*d*) J. Qian and F. Wu, *J. Mater. Chem. B*, 2013, **1**, 3464; (*e*) C. T. Huynh, M. K. Nguyen, J. H. Kim, S. W. Kang, B. S. Kim and D. S. Lee, *Soft Matter*, 2011, **7**, 4974; (*f*) Z. Xing, C. Wang, J. Yan, L. Zhang, L. Li and L. Zha, *Soft Matter*, 2011, **7**, 7992; (*g*) C. Ramkissoon-Ganorkar, A. Gutowska, F. Liu, M. Baudys and S. W. Kim, *Pharm. Res.*, 1999, **16**, 819; (*h*) Y. H. Lim, D. Kim and D. S. Lee, *J. Appl. Polym. Sci.*, 1997, **64**, 2647; (*i*) C. S. Brazel and N. A. Peppas, *J. Controlled Release*, 1996, **39**, 57; (*j*) G. Chen and A. S. Hoffman, *Nature*, 1995, **373**, 49.

7 (*a*) D. Klempner and K. C. Frisch, *Advances in Interpenetrating Polymer Networks*, Technomic, Lancaster, PA, 1994; (*b*) L. H. Sperling, *Interpenetrating Polymer Networks and Related Materials*, Plenum, New York, 1981.

8 (*a*) Z. M. O. Rzaev, S. Dincer and E. Piskin, *Prog. Polym. Sci.*, 2007, **32**, 534; (*b*) G. Zhang and C. Wu, *Adv. Polym. Sci.*, 2006, **195**, 101; (*c*) H. G. Schild, *Prog. Polym. Sci.*, 1992, **17**, 163; (*d*) H. Inomata, S. Goto and S. Saito, *Macromolecules*, 1990, **23**, 4887.

9 J. Zhang and N. A. Peppas, *J. Appl. Polym. Sci.*, 2001, **82**, 1077.

10 G. Staikos, K. Karayanni and Y. Mylonas, *Macromol. Chem. Phys.*, 1997, **198**, 2905.

11 J. Zhang and N. A. Peppas, *Macromolecules*, 2000, **33**, 102.

12 T. V. Burova, N. V. Grinberg, V. Ya. Grinberg, E. V. Kalinina, V. I. Lozinsky, V. O. Aseyev, S. Holappa, H. Tenhu and A. R. Khokhlov, *Macromolecules*, 2005, **38**, 1292.

13 (*a*) T. Swift, L. Swanson and S. Rimmer, *RSC Adv.*, 2014, **4**, 57991; (*b*) W. Zheng and L. He, *Biomater. Sci.*, 2014, **2**, 1471; (*c*) A. Aied, B. Glynn, H. Cao, Y. Zheng, H. Tai, A. Pandit and W. Wang, *Polym. Chem.*, 2012, **3**, 332; (*d*) X. Ji, Y. Yao, J. Li, X. Yan and F. Huang, *J. Am. Chem. Soc.*, 2013, **135**, 74.

14 F. M. Winnik, *Macromolecules*, 1990, **23**, 233.

15 Y. Shiraishi, R. Miyamoto, X. Zhang and T. Hirai, *Org. Lett.*, 2007, **9**, 3921.

16 (*a*) L. Tang, J. K. Jin, A. Qin, W. Z. Yuan, Y. Mao, J. Mei, J. Z. Sun and B. Z. Tang, *Chem. Commun.*, 2009, 4974; (*b*) B. Z. Tang, X. Zhan, G. Yu, P. P. S. Lee, Y. Liu and D. Zhu, *J. Mater. Chem.*, 2001, 2974; (*c*) J. Luo, Z. Xie, J. W. Y. Lam, L. Cheng, C. Qiu, H. D. Kwok, X. Zhan, Y. Liu, D. Zhu and B. T. Tang, *Chem. Commun.*, 2001, 1740.

17 (*a*) Z. Zhao, S. Chen, J. W. Y. Lam, P. Lu, Y. Zhong, K. S. Wong, H. S. Kwok and B. Z. Tang, *Chem. Commun.*, 2010, **46**, 2221; (*b*) V. S. Vyas and R. Rathore, *Chem. Commun.*, 2010, **46**, 1065.

18 (*a*) X. Shen, Y. Shi, B. Peng, K. Li, J. Xiang, G. Zhang, Z. Liu, Y. Cheng and D. Zhang, *Macromol. Biosci.*, 2012, **12**, 1583; (*b*) M. Wang, G. Zhang, D. Zhang, D. Zhu and B. Z. Tang, *J. Mater. Chem.*, 2010, **20**, 1858; (*c*) Y. Hong, H. Xiong, J. W. Y. Lam, M. Haessler, J. Liu, Y. Yu, Y. Zhong, H. H. Y. Sung, I. D. Williams, K. S. Wong and B. Z. Tang, *Chem. – Eur. J.*, 2010, **16**, 1232; (*d*) Y. Liu, Y. Tang, N. N. Barashkov, I. S. Irgibaeva, J. W. Y. Lam, R. Hu, D. Birimzhanova, Y. Yu and B. Z. Tang, *J. Am. Chem. Soc.*, 2010, **132**, 13951; (*e*) Y. Hong, M. Haeussler, J. W. Y. Lam, Z. Li, K. K. Sin, Y. Dong, H. Tong, J. Liu, A. Qin, R. Renneberg and B. Z. Tang, *Chem. – Eur. J.*, 2008, **14**, 6428; (*f*) T. L. Andrew and T. M. Swager, *J. Am. Chem. Soc.*, 2007, **129**, 7254; (*g*) S. J. Toal, K. A. Jones, D. Magde and W. C. Trogler, *J. Am. Chem. Soc.*, 2005, **127**, 11661.

19 (*a*) F. Mahtab, Y. Yu, J. W. Y. Lam, J. Liu, B. Zhang, P. Lu, X. Zhang and B. Z. Tang, *Adv. Funct. Mater.*, 2011, **21**, 1733; (*b*) M. Faisal, Y. Hong, J. Liu, Y. Yu, J. W. Y. Lam, A. Qin, P. Lu and B. Z. Tang, *Chem. – Eur. J.*, 2010, **16**, 4266; (*c*) W. C. Wu, C. Y. Chen, Y. Tian, S. H. Jang, Y. Hong, Y. Liu, R. Hu, B. Z. Tang, Y. T. Lee, C. T. Chen, W. C. Chen and A. K. Y. Jen, *Adv. Funct. Mater.*, 2010, **20**, 1413; (*d*) J. Liu, J. W. Y. Lam and B. Z. Tang, *J. Inorg. Organomet. Polym. Mater.*, 2009, **19**, 249; (*e*) S. Kim, H. E. Pudavar, A. Bonoiu and P. N. Prasad, *Adv. Mater.*, 2007, **19**, 3791.

20 (*a*) H. Zhou, J. Li, M. H. Chua, H. Yan, B. Z. Tang and J. Xu, *Polym. Chem.*, 2014, **5**, 5628; (*b*) H. Zhou, Q. Ye, W. T. Neo, J. Song, H. Yan, Y. Zong, B. Z. Tang, T. S. A. Hor and J. Xu, *Chem. Commun.*, 2014, **50**, 13785; (*c*) J. Li, J. Liu, J. W. Y. Lam and B. Z. Tang, *RSC Adv.*, 2013, **3**, 8193; (*d*) R. Hu, J. L. Maldonado, M. Rodriguez, C. Deng, C. K. W. Jim, J. W. Y. Lam, M. M. F. Yuen, G. Ramos-Ortiz and B. Z. Tang, *J. Mater. Chem.*, 2012, **22**, 232; (*e*) X.-M. Hu, Q. Chen, D. Zhou, J. Cao, Y.-J. He and B.-H. Han, *Polym. Chem.*, 2011, **2**, 1124; (*f*) J. Liu, Y. Zhong, P. Lu, Y. Hong,

J. W. Y. Lam, M. Faisal, Y. Yu, K. S. Wong and B. Z. Tang, *Polym. Chem.*, 2010, **1**, 426; (*g*) A. Qin, J. W. Y. Lam, L. Tang, C. K. W. Jim, H. Zhao, J. Sun and B. Z. Tang, *Macromolecules*, 2009, **42**, 1421.

21 (*a*) Z. M. O. Rzaev, S. Dincer and E. Piskin, *Prog. Polym. Sci.*, 2007, **32**, 534; (*b*) G. Zhang and C. Wu, *Adv. Polym. Sci.*, 2006, **195**, 101; (*c*) H. G. Schild, *Prog. Polym. Sci.*, 1992, **17**, 163; (*d*) H. Inomata, S. Goto and S. Saito, *Macromolecules*, 1990, **23**, 4887.

22 C. Tanford, *Physical Chemistry of Macromolecules*, John Wiley & Sons, New York, 1961, p. 550.

23 (*a*) D. Cai, Z. Wu, J. Jiang, Y. Wu, H. Feng, I. G. Brown, P. K. Chu and Z. Yu, *Sci. Rep.*, 2014, **4**, 3665; (*b*) Y.-S. Wu, Y.-C. Wu and S.-W. Kuo, *Polymers*, 2014, **6**, 1827; (*c*) J. Xu, C. L. Toh, X. Lu, S. Wang, C. He and X. Lu, *Macromolecules*, 2005, **38**, 1684; (*d*) J. Xu, C. He, K. C. Toh and X. Lu, *Macromolecules*, 2002, **23**, 8846.